Thermal Mapping of Hollow Cathodes to Model the Thermal Loads of Iodine Ion Propulsion

Paul Winner¹

Embry-Riddle Aeronautical University, Daytona Beach, Florida, 32114, United States

Kirk J. Boehm² and Richard D. Branam³

The University of Alabama, Tuscaloosa, Alabama, 35401, United States

Iodine possesses desirable qualities that could make it a potential fuel of choice in future space missions requiring ion propulsion, potentially replacing Xenon; if the thruster can have similar endurance despite Iodine's corrosiveness. A computer-aided design model of a hollow cathode with a Lanthanum Hexaboride insert was created in Solidworks, using its thermal load simulator to generate an approximate temperature model of it in operation. Data was then collected to refine the model by getting temperature readings of a hollow cathode in operation by attaching type K thermocouples to the outside and inside of the hollow cathode and firing it in a vacuum chamber. Differences between the thermal model and the experimental data will be discussed in addition to the assumptions made within the thermal model. Based on the data, the hollow cathode is far below expected temperatures, though there are several sources of error to explain this discrepancy.

Nomenclature

 c_v = Isobaric Heat Constant

D = Pipe Diameter

 E_b = Thermal Radiation Flux

g = Gravitational acceleration of earth

h = Enthalpy

 I_D = Anode Current

 I_K = Keeper Current

k = Boltzmann Constant

L = Pipe Length

Nu = Nusselt's Number

p =Static Pressure

 P_R = Plasma radiative term

Pr = Prandtl's Number

¹ NSF Undergraduate Researcher, Student Member

² Doctoral Student, Department of Aerospace Engineering and Mechanics.

³Assistant Professor Department of Aerospace Engineering and Mechanics

r = Radial coordinate

Re = Reynold's Number

Sccm= Standard cubic centimeters per minute

u = Axial velocity component

v = Radial velocity component

x = Axial coordinate

 $\mu = Dynamic viscosity$

 $\rho = Density$

 σ = Stefan-Boltzmann constant

 $\varepsilon = \text{Emissivity}$

I.Introduction

HOLLOW cathodes have been a principal part of electric space propulsion since its inception. In short, the goal of a hollow cathode is to neutralize the ions coming out of the main thruster in the propulsion system using a thermally generated plasma; typically, around 1275-1650 °C. The cathode temperature depends on the mass flow rate, current of the plasma and the distance from the orifice entrance according to Polk et al. [1]. The cathodes function is to prevent the ions from being forced back to the spacecraft by electrostatic forces. As the charged ions exit the propulsion system, the spacecraft net charge is negative. The cathode asks as a ground, ejecting electrons to keep the spacecraft neutral (grounded). The performance, capabilities, and longevity of any electric propulsion system can be surmised by studying the characteristics of a hollow cathode. Any research able to offer prediction or improvement into any of these characteristics is of a high degree of significance. Being able to reasonably predict the thermal behavior of the cathode plasma provides a valuable design tool to spacecraft companies. To best capture the physical processes, some assumptions are warranted. Assuming the temperature distribution across the cathode is significant provides bounds for our expected results. [1] [2] The plasma radiation is an appreciable fraction of the heat released, making it a significant source of the temperature difference [3]. A combination of both CAD models of a hollow cathode and experimental data from type C thermocouples attached to both the outside and the inside of the hollow cathode were utilized to use thermal behavior as a predictor of plasma behavior. This experiment had the following objectives:

- Gain a sufficient understanding of the range of temperatures that can be expected for hollow cathodes of similar caliber and the mechanisms of both the heat and plasma behavior.
- 2. Create an accurate model of a hollow cathode using Solidworks with some basic thermal constraints to predict normal operating thermal conditions within the cathode.
- 3. Prepared thermocouples and the DAQ system to protect them against the arcing of the plasma using op amps, developed a LABVIEW program, tested the setup, setup power lines and feedthroughs, setting up

the hollow cathode, in addition to other preparation tasks prior to igniting the hollow cathode for data collection.

- 4. Calibrate, attach and test thermocouples on a hollow cathode and verify the thermocouples yield expected temperatures under normal operating conditions.
- 5. Using experimental data from ignition the hollow cathode to compare to the initial thermal model. Adjust the Solidworks model to best predict the temperature of the cathode (goal is within \pm 5 K)

II. Hollow Cathode Setup

The hollow cathode performance for this experimentation, shown in Figure 1, has been well documented by previous researchers at the University of Alabama. One key thing to note about Figure 1, the hollow cathode ran in a heaterless, open configuration; the cathode relied solely on the current from the keeper and anode power supplies to start the cathode. The heat needed to maintain plasma production in the cathode was then self-generated.

The molybdenum cathode, is 75.5 mm long, with an 8.51 mm outer diameter and a 7.11 mm orifice diameter at

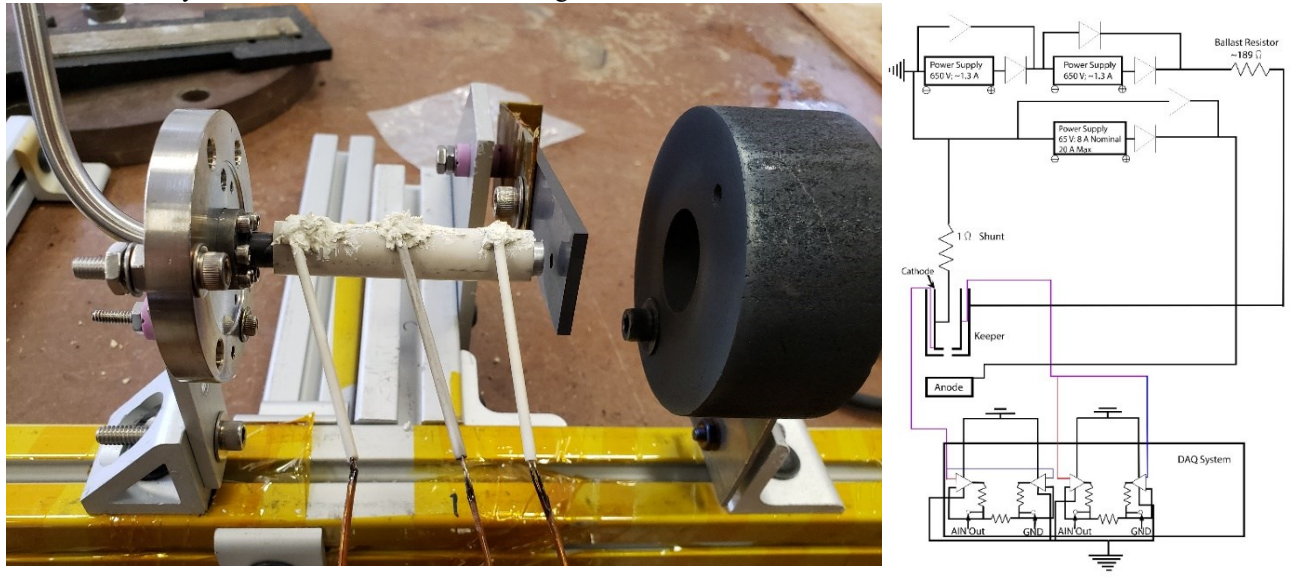


Figure 1: An image of the complete hollow cathode setup, just prior to insertion into a vacuum chamber, the keeper is immediately to the right of the cathode, with the on the far right.

Add another figure for the wireframe drawing of the cathode/keeper/anode. Identify each of the major parts in the figure.

the end The orifice, made from tantalum has a 5.92 mm outer diameter and 1.96 mm inner diameter, with 0.23 mm thick. The keeper and anode are made from graphite. The keeper is approximately 75 mm long by 21 mm wide, with an approximately 3.0 mm diameter orifice for plasma to pass through. The spacing between the keeper and the cathode is 1.0 mm at all times, and the distance between the anode and the cathode is approximately 25.4 mm at all times.

Data was captured at two keeper/cathode configurations; 1.0 mm and a 2.0 mm. Among other key parts of the test stand include the ceramic spacers, used at all locations where electrical current was needed to flow to get the hollow cathode running. The spaces ensured the applied electrical power was isolated from the entire vacuum chamber. So, the ceramic spacers were used to isolate the anode, keeper, and cathode from the entire test stand. The test stand itself was constructed from extruded aluminum. All three parts of the hollow cathode rested on before it was mounted in the vacuum chamber using the same aluminum test stand. The gas was fed into the cathode remained leak tight. A leak out into the chamber could cause arcing and higher than space-like pressures. A gas flow isolator made of threaded pink alumina was used at the site of the feedthrough, before connecting to the hollow cathode piping.

The chamber itself is an Ion Tech Beam System vacuum chamber 0.457 m in diameter and 0.914 m in length. Space-like pressures (10⁻⁶ torr) is generated by flowing cryogenically cooled liquid helium through the system. Once a roughing pump pumps the chamber down from its initial atmospheric pressure of 760 torr down to around 760 millitorr, the cryopump used to cool the helium is opened, freezing out the gas, allowing the chamber to reach the desired pressure. Gas inflow was controlled via mass flow controllers rated to 25 sccm for nitrogen gas. When corrected for argon, the flow rate is 40 sccm. Two power supplies were used in series to power the keeper, a Lambda GEN600-1.3 and a Lambda X+650-1.25. For the anode, a Lambda GEN60-25 was used. The power supplies are protected by RURG80100 diodes from potential backflow of electricity Due to some unforeseen consequences, we used at least three different data acquisition (DAQ) system. Initially, the DAQ was protected by an op-amp circuit in the case of arcing. The op-amp circuit was removed from the system because of signal/ground loop issue. The issue was more pronounced than realize, damaging the primary and a spare LabJackT7 DAQ. As a backup, a Fluke 287 multimeter was used, with a max DAQ rate of 1 Hz.

The thermocouples themselves are located in three positions; far upstream on the cathode around 20 mm from the base, well before any ignition of the Argon gas has taken place, and another was placed around 43 mm from the cathode base. This sensor placement will capture more data on the cathode temperature prior to gas ignition, but further downstream to better map areas closer to the heat source. The final thermocouple was located at 60 mm from the cathode base right above where the insert is located, Argon gas is "ignited" into plasma. This sensor will directly indicate properties of the plasma inside the cathode. These thermocouples were initially three type C thermocouples,

attached via ceramic paste aligned axially with the cathode. This configuration allows the keeper "shroud" to cover the cathode and the thermocouples. This original method of thermocouple alignment is displayed in Figure 2.



Figure 2: Due to the extreme amount of heat released in the process of firing the cathode, the ceramic paste used to keep the thermocouples in place would consistently remove itself from the cathode.

The thermocouples kept detaching themselves from the cathode. In the process of reattaching the type C thermocouples, all were damaged. Available type K thermocouples were substituted since they operate in a similar temperature range. The "closed" configuration of the cathode could no longer be used, since the type K thermocouples were simply of a gauge size too small to fit within the confines of the "closed" keeper shroud. Instead, the thermocouples were aligned perpendicular to the cathode in an open configuration. The entire system was automated to run remotely via a computer. All input and control variables (mass flow, pressure, keeper and anode current/voltage) were monitored and set on the same system with the data recording to ensure the information was synchronized.

III. Literature Research & Background

When the creation of the thermal model was started, of key importance was to know just how plasma behaves in heat transfer through all the classic mechanisms of heat transfer. Utilizing data gathered by Polk [1], we found the ranges of temperatures that a hollow cathode of similar composition and current ranges has throughout said cathode. We also looked into the behaviors that low-energy plasma has when it comes to heat transfer, specifically Argon plasma. According to Incropera and Leppert [3], the two primary means of heat transfer for such a plasma would be convection and radiation when going through a circular pipe, which is of great resemblance to a hollow cathode.

Incropera and Leppert also derived several equations of heat transfer for said Argon plasma, assuming axisymmetric and steady flow, both of which are applicable to our hollow cathode as the Argon gas flow is controlled via a mass flow controller, and given the extremely low flow rates on the order of cm³ per minute (sccm), the flow is assumed to be laminar, and thus axisymmetric, meaning their derived equations can apply to our model of hollow cathode heat transfer. Given these assumptions, as listed by Incropera and Leppert, the boundary layer equations become Equations 1, 2, and 3.

$$\frac{\partial}{\partial x}(\rho u) + \frac{1}{r}\frac{\partial}{\partial r}(r\rho v) = 0 \quad (1)$$

$$\rho\left(u\frac{\partial u}{\partial x} + v\frac{\partial u}{\partial r}\right) = -\rho g - \frac{dp}{dx} + \frac{1}{r}\frac{\partial}{\partial r}\left(r\mu\frac{\partial u}{\partial r}\right) \quad (2)$$

$$\rho\left(u\frac{\partial h}{\partial x} + v\frac{\partial h}{\partial r}\right) = u\frac{dp}{dx} + \frac{1}{r}\frac{\partial}{\partial r}\left(r\frac{k}{c_n}\frac{\partial h}{\partial r}\right) + \mu\left(\frac{\partial u}{\partial r}\right)^2 - P_R \quad (3)$$

There are three key terms in these relationships normally are neglected but are significant for thermal plasma: plasma radiation term, radial convective term, and the viscous dissipation. Incropera and Lepptert \ll just reference them \gg The plasma radiation term, P_R can have a significant effect on the temperature characteristics of the plasma moving through the hollow cathode. The radial convective term comes from the momentum equation. The radial convection term affects the development of the plasma's velocity along the hollow cathode. The viscous dissipation term $\left(\mu\left(\frac{\partial u}{\partial r}\right)^2\right)$ models the effect to both the velocity and the convection of the thermal plasma. When trying to capture heat transfer in a convecting system [4] the Nusselt number is paramount for laminar hot gases, including plasmas, for predicting heat behavior. The Nusselt number is a function of both the fluid's Reynolds number and Prandtl number. Such a relation is described within Equation 4.

$$Nu_D = 3.66 + \frac{0.065*Re*Pr*\frac{D}{L}}{1+0.04*\left(Re*Pr*\frac{D}{L}\right)^{\frac{2}{3}}}$$
(4)

This number characterizes the relative magnitudes = of the plasma's convective vs. conductive rates of heat transfer. $Nu_D \sim 1.0$ equats to pure conduction. Values between 1.0 and 10 represent laminar flow convection. Values above 10 represent convection from turbulent flow [5]. Pfender determined that for a laminar flow plasma, the Nusselt number is 3.66 Plasma also contributes a significant amount of radiative heat transfer to the surrounding area, which follows Stefan-Boltzmann's law of radiative transfer, seen in Equation 5. Reference Gleizes [xx]

$$E_b(T) = \epsilon \sigma T^4 \tag{5}$$

For many cases, the radiation of the plasma to the surrounding surface is negligible. The radiation intensity increases both with temperature and pressure within the temperature ranges of around 8,000-30,000 K (1.0 to 2.0 eV) at the core of the plasma, a typical low energy thermal plasma [4][5]. Radiation intensity decreases as pressure decreases. At lower pressures, radiation will decrease. Plasma's primary method of heat transfer is through radiative measn. Heat cannot be wicked away solely through conduction or convection [4].

IV.Setup & Heat Transfer Model

The first task of this experiment was to create a preliminary heat transfer model and its corresponding temperature distribution within a hollow cathode. The two largest forces at work in the heat transfer are the convection and radiation of the plasma in the hollow cathode. Convection is increasingly important further downstream in the hollow cathode. We grounded our model using previous temperature measurements from Polk et al. [1] to create a temperature distribution of the hollow cathode experimented on, shown in Figure 3.

Magin same Circuits Model (Amongs) (1.7)
2009 (passimants) (1.7)
2019 (1.7)
2019 (1.7)
2019 (1.7)
2019 (1.7)
2019 (1.7)
2019 (1.7)
2019 (1.7)
2019 (1.7)
2019 (1.7)
2019 (1.7)
2019 (1.7)
2019 (1.7)
2019 (1.7)
2019 (1.7)
2019 (1.7)
2019 (1.7)
2019 (1.7)
2019 (1.7)
2019 (1.7)
2019 (1.7)
2019 (1.7)
2019 (1.7)
2019 (1.7)
2019 (1.7)
2019 (1.7)
2019 (1.7)
2019 (1.7)
2019 (1.7)
2019 (1.7)
2019 (1.7)
2019 (1.7)
2019 (1.7)
2019 (1.7)
2019 (1.7)
2019 (1.7)
2019 (1.7)
2019 (1.7)
2019 (1.7)
2019 (1.7)
2019 (1.7)
2019 (1.7)
2019 (1.7)
2019 (1.7)
2019 (1.7)
2019 (1.7)
2019 (1.7)
2019 (1.7)
2019 (1.7)
2019 (1.7)
2019 (1.7)
2019 (1.7)
2019 (1.7)
2019 (1.7)
2019 (1.7)
2019 (1.7)
2019 (1.7)
2019 (1.7)
2019 (1.7)
2019 (1.7)
2019 (1.7)
2019 (1.7)
2019 (1.7)
2019 (1.7)
2019 (1.7)
2019 (1.7)
2019 (1.7)
2019 (1.7)
2019 (1.7)
2019 (1.7)
2019 (1.7)
2019 (1.7)
2019 (1.7)
2019 (1.7)
2019 (1.7)
2019 (1.7)
2019 (1.7)
2019 (1.7)
2019 (1.7)
2019 (1.7)
2019 (1.7)
2019 (1.7)
2019 (1.7)
2019 (1.7)
2019 (1.7)
2019 (1.7)
2019 (1.7)
2019 (1.7)
2019 (1.7)
2019 (1.7)
2019 (1.7)
2019 (1.7)
2019 (1.7)
2019 (1.7)
2019 (1.7)
2019 (1.7)
2019 (1.7)
2019 (1.7)
2019 (1.7)
2019 (1.7)
2019 (1.7)
2019 (1.7)
2019 (1.7)
2019 (1.7)
2019 (1.7)
2019 (1.7)
2019 (1.7)
2019 (1.7)
2019 (1.7)
2019 (1.7)
2019 (1.7)
2019 (1.7)
2019 (1.7)
2019 (1.7)
2019 (1.7)
2019 (1.7)
2019 (1.7)
2019 (1.7)
2019 (1.7)
2019 (1.7)
2019 (1.7)
2019 (1.7)
2019 (1.7)
2019 (1.7)
2019 (1.7)
2019 (1.7)
2019 (1.7)
2019 (1.7)
2019 (1.7)
2019 (1.7)
2019 (1.7)
2019 (1.7)
2019 (1.7)
2019 (1.7)
2019 (1.7)
2019 (1.7)
2019 (1.7)
2019 (1.7)
2019 (1.7)
2019 (1.7)
2019 (1.7)
2019 (1.7)
2019 (1.7)
2019 (1.7)
2019 (1.7)
2019 (1.7)
2019 (1.7)
2019 (1.7)
2019 (1.7)
2019 (1.7)
2019 (1.7)
2019 (1.7)
2019 (1.7)
2019 (1.7)
2019 (1.7)
2019 (1.7)
2019 (1.7)
2019 (1.7)
2019 (1.7)
2019 (1.7)
2019 (1.7)
2019 (1.7)
2019 (1.7)
2019 (1.7)
2019 (1.7)
2019 (1.7)
2019 (1.7)
2019 (1.7)
2019 (1.7)
2019 (1.7)
2019 (1.7)
2019 (1.7)
2019 (1.7)
2019 (1.7)
2019 (1.7)
2019 (1.7)
2019 (1.7)
2019 (1.7)
2019 (1.7)
2019 (1.7)
2019 (1.7)
2

Figure 3: The primary mechanisms of heat transfer in this simulation are constant temperature constraints at the insert and orifice plate

and convective heat transfer throughout the cavity.

The verified model follows experimental results well. [1] The experimental setup for measuring the temperature of the hollow cathode was then grounded to the model. We first took three type K thermocouples and calibrated them via using boiling and freezing water to create a T_{actual} vs. T_{measured} plot. In order to protect the DAQ system, an operational-amplifier circuit was created and linked with the type K thermocouples⁴. A schematic of the operational amplifier circuit is shown in Figure 3.

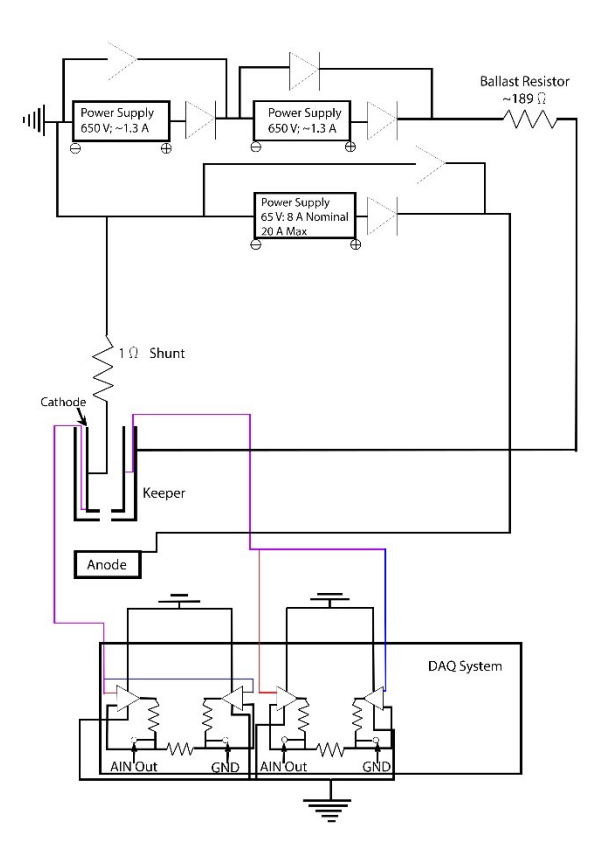


Figure 4:-All power supplies are surrounded by diodes for protection.-The bottom rectangle represents the DAQ system with op-amp circuits for protection against abnormal voltage spikes.

After calibration, each thermocouple was secured to the cathode with an alumina ceramic tube sealed with ceramic paste at distances 19, 43, and 60 mm from the cathode plate. The hollow cathode was secured to a test stand, shown in Figure 4, and placed in a vacuum chamber Once the vacuum chamber reached 10⁻⁶ torr, argon is allowed to flow in before igniting it into plasma via the power supplies shown in the schematic in Figure 2.

⁴ The operational-amplifier setup was first tested on a single thermocouple to see if a linear thermocouple relation was still retained with the added circuitry.



Figure 5: Above is a picture of the setup of three type K thermocouples on a hollow cathode in an "open" configuration.

Once the argon flow was initiated and before ignited into plasma, the DAQ system recorded thermal data on the cathode via a LABVIEW program. Both transient and steady-state thermal data were captured for the hollow cathode on the following conditions noted in Table 1.

Case	ṁ	ID	IK	Anode	Keeper	Orifice	Chamber
				Spacing	Spacing		Pressure
-	scem	A	A	mm	mm	mm	torr
1a	5	1	1.312	25.4	2	2	1-4*10-4
1b	5	2	1.312	25.4	2	2	1-4*10-4
1c	5	4	1.312	25.4	2	2	1-4*10-4
1d	5	6	1.312	25.4	2	2	1-4*10-4
2a	6	1	1.312	25.4	2	2	1-4*10-4
2b	6	2	1.312	25.4	2	2	1-4*10-4
2c	6	4	1.312	25.4	2	2	1-4*10-4
2d	6	6	1.312	25.4	2	2	1-4*10-4
3a	8	1	1.312	25.4	2	2	1-4*10-4
3b	8	2	1.312	25.4	2	2	1-4*10-4
3c	8	4	1.312	25.4	2	2	1-4*10-4
3d	8	6	1.312	25.4	2	2	1-4*10-4
4a	10	1	1.312	25.4	2	2	1-4*10-4
4b	10	2	1.312	25.4	2	2	1-4*10 ⁻⁴

4c	10	4	1.312	25.4	2	2	1-4*10 ⁻⁴
4d	10	6	1.312	25.4	2	2	1-4*10 ⁻⁴
5a	12	1	1.312	25.4	2	2	1-4*10 ⁻⁴
5b	12	2	1.312	25.4	2	2	1-4*10-4
5c	12	4	1.312	25.4	2	2	1-4*10 ⁻⁴
5d	12	6	1.312	25.4	2	2	1-4*10-4
6a	13	1	1.312	25.4	2	2	1-4*10-4
6b	13	2	1.312	25.4	2	2	1-4*10-4
6c	13	4	1.312	25.4	2	2	1-4*10-4
6d	13	6	1.312	25.4	2	2	1-4*10 ⁻⁴
7a	15	1	1.312	25.4	2	2	1-4*10-4
7b	15	2	1.312	25.4	2	2	1-4*10 ⁻⁴
7c	15	4	1.312	25.4	2	2	1-4*10 ⁻⁴
7d	15	6	1.312	25.4	2	2	1-4*10-4
8a	20	1	1.312	25.4	2	2	1-4*10 ⁻⁴
8b	20	2	1.312	25.4	2	2	1-4*10-4
8c	20	4	1.312	25.4	2	2	1-4*10-4
8d	20	6	1.312	25.4	2	2	1-4*10-4

Table 1: The above list is the list of all scenarios we went through in testing the cathode and finding its temperature distribution.

The temperature results were compared to the initial thermal model to assess its validity. The critical unknown value is the plasma temperature. We guessed an initial value for the model initial. The measured results now gave us a way to predict the plasma temperature. Once calibrated with the data, the thermal model was within $\pm 5\%$ of the actual temperature readings. We then recorded the conditions for the thermal model to bring about these predictive behaviors in order to later apply them to various plasmas, not just argon.

V. Results

here were two trends are apparent in the temperature data. As the current to the anode increased, so did the overall temperature of the cathode, becoming visibly brighter, as shown in Figure 4. Increasing mass flow increased cathode temperature. Again, this change brought a noticeable increase in brightness of the cathode, shown in Figure 5.

<< move to earlier in the paper >> During the calibration process, the op-amp circuit had no bearing on the linearity of a thermocouple's calibration process. << plot this data >>

Thermocouple TC1 Temperature	Thermocouple TC1 Voltage
0.464	-0.001093067
0.643	-0.00108806

0.875064916	-0.001079699
1.086978236	-0.00107
0.983088344	-0.001075663
Average: 0.810429467	Average: -0.001081655

Table 2: An overview of one of the thermocouples list of registered temperatures and corresponding voltages for the calibration process at 0°C.

<< move to earlier (where talking about the process and setup) with the paragraph above >> Temperature readings exhibited significant amounts of noise in the thermocouples upon ignition of the plasma. This is Possible causes considered were the large temperature differences between the cathode and the ceramic mounting tube for the thermocouples, or the plasma itself inducing an emf on the thermocouple, yielding a false value. >>

Results for the temperature of the hollow cathode were way below expected values by several hundred degrees Celsius, peaking at around a 600°C average as shown in Table 3. This is The large difference is obviously not representative of the actual conditions for the cathode. Much of the cathode is visibly glowing an orange-yellow, as shown in Figures



Figure 6: The hollow cathode being fired with an anode current of 1 A.-Note that the dark streak on the right is the thermocouple and Nickel-Chromium wires securing the thermocouples to the cathode.

5 and 6. Spectral techniques suggest the cathode has entered the incandescent stages of thermal radiation, well beyond the thermocouple's measurement range.

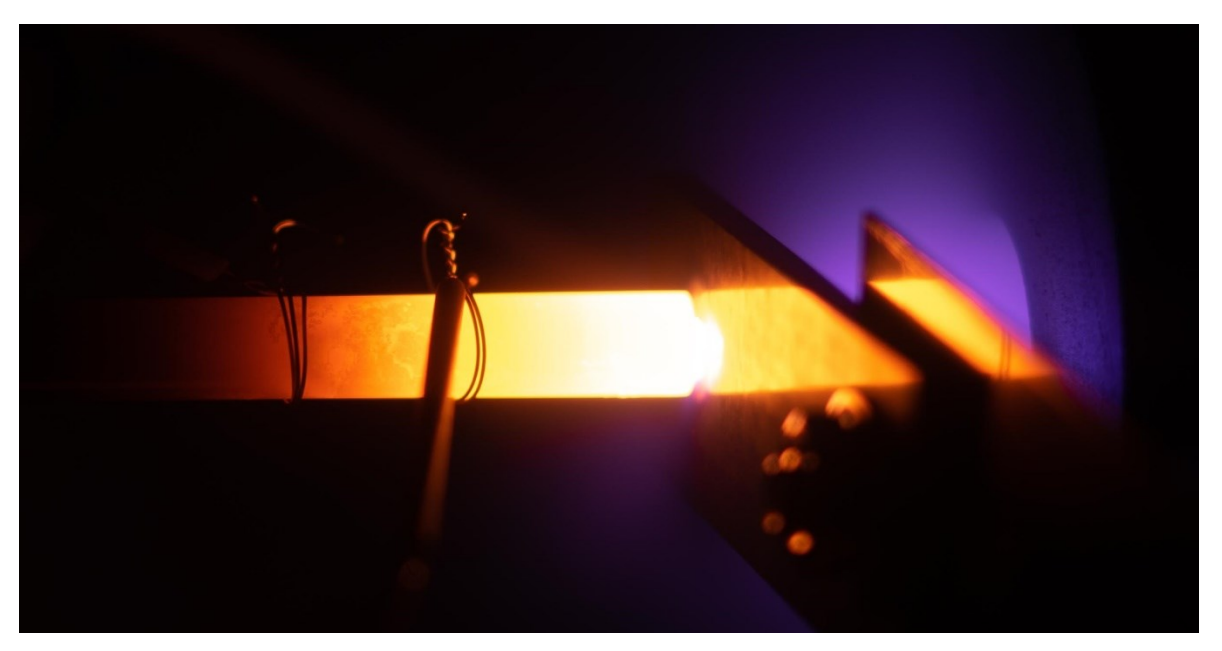


Figure 7: The hollow cathode being fired with an Anode current of 6 A.-Note that the purple glow is the Argon plasma flowing to the Anode.

Our result confirms the model's prediction, showing thermal radiation becomes an increasing factor of the thermal properties of the hollow cathode the further downstream. Our data showed a lower temperature at the insert than at the middle of the cathode, with the temperature cooling off near the end, as evidenced in Table 3. The obviously incorrect physical trend could potentially be an induced electromagnetic fluctuation from the plasma coupled with insulation effects from the ceramic coating on the thermocouple. The ceramic paste and alumina casing would normally insulate the tip from any electromagnetic fluctuations, but the plasma is very conductive and can form throughout the entire test chamber. The front thermocouple is being thermally insulated from the cathode adding to the erroneous readings.

For the middle downstream thermocouple, the temperatures recorded by the data acquisition system were far higher, hovering around 620-650 °C. The insulation is causing significant error due to the ceramic coating surrounding the thermocouple. The thermocouple results furthest downstream can be compared with temperatures representative of the incandescence. The metal should be glowing as shown in Figures 4 and 5. One further potential source of error that was discovered upon removal of the cathode from the chamber was that some of the thermocouples weren't actively touching the cathode's surface, thus creating an erroneous reading. One problem that was consistent with

taking data readings was the errors thrown by multiple DAQ systems upon starting data collection. What would appear would be a large spike in recorded temperature, followed by a flatline. Presumably, this was a surge of voltage going through the DAQ system would cause it to automatically shut itself off from further data readings for further protection. We could not overcome the persistent issues with the automated DAQ system. A Fluke 287 was used to record the temperature data, as shown in Figure 6. A plot for each thermocouple in cases 3 and 4 are shown in Figures 7-12 to show case the general behavior of the cathode's temperature at each point. The further cases are in the Appendix.

VI.Conclusion

The complexity of a hollow cathode can be achieved by eliminating the heater from the system, as the cathode is capable of igniting sans heater at high mass flow rates (~25 sccm) and at modest anode currents (~2 A). The thermocouple's sensitivity to plasma is apparent. For The thermocouples need to be sufficiently isolated them from the plasma. Thermocouples that have with a higher temperature ceiling will also be useful in ensuring that the upper limit temperature readings are believable. A secondary verification system will also prove useful in ensuring that the thermocouples are providing an accurate temperature readout. The significant error discovered in our result provided valuable conclusions as well. Thermocouples need to be shielded from the plasma and the rest of the system. Touching insulating materials like the ceramic tubing will result in much lower temperature readings. The thermocouple reading is being influenced by both sources of heat. The thermocouples are extremely sensitive to a plasma-dominated environment was A significant amount of noise was generated by the thermocouples in the vacuum chamber as the cathode was firing. Further investigation is definitely needed to find all the sources of this noise and then eliminate them. The DAQ systems need protected circuitry to ensure they are not damaged. Two LabJack DAQ systems broke as a result of the cathode arcing to the thermocouples. Op-amp systems do appear to be a solid solution, but an appropriate circuit needs to be designed for our equipment. During the experiment, our op-amps failed to amplify the signal linearly.

Funding Sources

Funding for this research was provided by the NSF REU Grant #1659710.

Acknowledgments

This work is supported by the NSF Grant \#1659710 and the NSF EPSCoR RII-Track-1 Cooperative Agreement OIA-1655280

References

- [1] Polk, J., Goebel D., and Guerrero P., "Thermal Characteristics of a Lanthanum Hexaboride Hollow Cathode," 30th ISTS and 6th NSAT Joint Conference, Hyogo-Kobe, Japan, 2015, IEPC-2015-44/ISTS-2015-b-44.
- [2] Polk, J., Marrese, C., Thornber, B., Dang, L., and Johnson, L., "Temperature Distribution in Hollow Cathode Emitters," 2004 Joint Propulsion Conference, Fort Lauderdale, FL, July, 2014, AIAA-2004-4116.
- [3] Incropera, F. and Leppert, G., "Laminar Flow Heat Transfer from an Argon Plasma in a Circular Tube," Int. J. Heat Mass Transfer Paper, Vol. 10, pp. 1861-1873, Stanford, California, July 1967.
- [4] Pfender, E., "Heat Transfer from Thermal Plasmas to Neighboring Walls or Electrodes," Pure & Applied Chemistry Paper, Vol. 48, pp. 199-213, Minneapolis, MN, 1976.
- [5] Gleizes, A., "Radiative Plasma Heat Transfer," Handbook of Thermal Science and Engineering, edited by F.A. Kulacki, Springer Nature 2018, 2018, pp. 2600-2652.

doi: 10.1007/978-3-319-26695-4 26